Supplementary Information

Kinematics and kinetics of reaching movements. Figure S1 illustrates kinematic and kinetic features of reaching movements performed in a horizontal plane, in each of the four load conditions (NL, VS, VE, and VB). Data shown are from monkey A. Figure S1a shows mean hand paths for movements to 8 targets from a central start position. Figure S1b-e shows data for movements to the forward target (bold circle in Figure S1a). Figure S1b and S1c show associated joint angles and velocities for the shoulder and elbow; increasing values indicate flexion, decreasing values indicate joint extension. Figure S1d shows time-varying torque applied at the shoulder and elbow by the KINARM device, and Figure S1e shows muscle torque (computed using inverse dynamics[1]) generated by the monkey in each load condition.

The robotic device is designed such that motor 1 applies loads at the shoulder while motor 2 applies loads at both the shoulder and elbow joints[1]. In order to generate a viscous load at the elbow, motor 1 and motor 2 are programmed to generate loads of equal magnitude but opposite in sign. Any difference in the magnitude of torque generated by the motors creates an unintended load at the shoulder (cross-talk) when a load is applied to the elbow (VE task). We computed the magnitude of this cross-talk for the VE task by computing the absolute difference in torque generated by each motor at peak hand velocity for movements recorded from monkey A and B. The absolute difference in torque applied by the two motors (i.e. unintended load at the shoulder) was small ($3.6 \pm 2.5\%$ of the load applied to the elbow [mean and sd]).

Even though peak hand velocity was similar for all movement directions[2], peak angular velocity at each joint variedly strongly with movement direction (Figure S2a).

Movements away and towards the monkey required larger angular velocies than movements to the left and right. Correspondingly, the magnitude of the velocity-dependent loads applied to each joint varied in a similar manner with movement direction.

Figure S2b illustrates the directional tuning of cells across the population in the NL condition. All cells with a statistically significant PD (bootstrap, p<0.01) are shown. Each dot represents a single cell, and is plotted along the cell's PD. The distribution of PDs for unloaded reaching was not uniform when compared to a bimodal distribution (P<0.001, main axis = 106-286 , Fig. S2b). Our previous report, with a much larger sample of cells, illustrated that this bias in the distribution correlated better with joint power than with joint velocity (See Ref. #2). Figure S2c illustrates the directional tuning, in the NL condition, of the subset of cells which were sensitive to at least one of the three viscous loads. The distribution of PDs was also found to be non-uniform as compared to a bimodal distribution (P<0.001, main axis = 107-287 , Fig. S2c). Distributions of PDs for each load condition were quite similar and indistinguishable given the small sample sizes.

Despite the large changes in the kinetic features of movement in VS, VE and VB the monkeys were successful in holding the kinematics constant across load conditions. Statistical tests were conducted on a number of kinematic features of movement to assess the level of kinematic consistency across the different load conditions. As a proportion of the total movements recorded in NL and in at least one load condition, only a very small number showed significant differences for the following kinematic variables – hand movement distance: 3% of cases; peak hand tangential velocity: 2%; movement speed: 2%; linearity ratio[3]: 3%. Moreover in the majority of these cases the differences were small, less than 10% of the mean values. This kinematic control is crucial as it allows differences observed in cell activity across the different load

conditions to be ascribed to changes in kinetic, rather than kinematic features of movement.

Possible time-dependent changes in neural activity. As a control for time-dependent changes in cell activity, the monkeys made movements in the NL condition a second time, once all the viscous load conditions had been collected. This control test was recorded in 97 cells (monkey A: 37; monkey B: 20; monkey C: 40). Of those 97 cells, significant differences in mean neural discharge between the first and last NL blocks were observed in only 17 cells ($p<.05$, ANOVA) (monkey A: 4; monkey B: 4; monkey C: 9). These 17 cells were excluded from the analyses reported here.

Electromyography of forelimb muscles. In each monkey, the electromyographic (EMG) activity of up to 16 forelimb muscles was recorded during the no-load condition (NL) and during each of the three viscous load conditions (VB, VS, VE). Mono- and bi-articular muscles spanning the shoulder and elbow were sampled, including Long (LB) and Short (SB) heads of Biceps, Brachialis (B), Brachioradialis (Br), Anterior (AD), Middle (MD) and Posterior (PD) heads of deltoids, Dorsoepitrochlearis (De), Infraspinatus (I), Pectoralis Major (PM), Subscapularis (Sb), Supraspinatus (Sp), Teres Major (TM), and Lateral (LaT), Long (LoT) and Medial (MT) heads of Triceps. Pairs of single-strand wires were inserted percutaneously in monkeys A, B and C, and pairs of multi-strand wires were implanted chronically in monkeys A and C under aseptic conditions[2,4,5]. In monkeys A and C some muscles were sampled twice, once using chronically implanted wires and a second time using percutaneously inserted wires providing a total of 57 samples of EMG. Electrode placement was verified using microstimulation.

Of the 57 muscles sampled, 55 changed activity as compared to NL in at least one of the three loads. Fifty EMGs responded to either VS or VE with 25 of these responding to both loads. Forty-nine EMGs changed their activity for VB and 44 of

these responded to either VS or VE. Ninety-seven of the 125 statistically significant observations across the three load conditions reflected an increase rather than a decrease in discharge from the NL condition. Table S1 illustrates the number of significant observations where the muscles are divided into three groups: 1) primary mono-articular muscles at the shoulder, 2) Bi-articular muscles spanning shoulder and elbow, and 3) Mono-articular muscles at the elbow.

As shown in our previous work[6], muscles spanning one joint often changed their activity for loads applied to the other joint (see also Ref. #7 and 8). While many mono-articular muscles responded to loads at both joints, the relative effect of loads tended to be larger at the spanned as compared to the non-spanned joint. We scored the response of shoulder and elbow mono-articular muscles for loads at each joint based on the equation,

$$Score = 1 - (|\_VS| - |\_VE|)/(2*(sqrt(\_VS^2 + \_VE^2))), \tag{1}$$

where _VS and _VE equal the maximal change in activity for VS and VE loads for each cell relative to its activity for unloaded reaching movements across all movement direction. A score of 0 means that the muscle only changed its activity for loads at the elbow and a score of 1 means it only changed its activity for loads at the shoulder. The average score for elbow muscles (0.320 ± 0.053; mean $\pm$ SEM) was significantly smaller than the average score for shoulder muscles (0.576 ± 0.047; t-test, $p<0.001$).

Figure S1. Kinematic and kinetic characteristics of reaching movements in a horizontal plane. **a**: Hand trajectories to 8 visual targets from a central start position, for four load conditions:no-load (NL), VS, VE and VB. **b**: Time-varying joint angles for a single reaching movement to the forward target (target shown in bold in **a**), for the four load conditions. **c**: Joint velocities. **d**: Torques applied to the shoulder and elbow by KINARM. Torque values are converted into joint

loads where shoulder torque equals motor torque 1 plus motor torque 2 and elbow torque equals motor torque 2 (See Ref. 1). **e**: Muscle torques at the shoulder and elbow computed using inverse dynamics. Mean data are shown from monkey A; increasing values indicate joint flexion. All signals are aligned to movement onset (time=0).

Figure S2. **a**: Variations in peak joint velocity for movements in different directions for shoulder (red), elbow (blue) and the largest summed value (green). **b**: Distribution of PDs for all cells based on activity during NL condition (bootstrap p<0.01). Each circle represents the directional preference of an individual cell and cells are grouped into 16 equal-sized bins (bin_size = 22.5). As in our previous work that represented a larger sample of cells (including the present ones), the distribution was not uniformly distributed as compared with a bimodal distribution. **c**: Distribution of PDs in the no-load condition for cells sensitive to at least one of the three load conditions, and having a significantly tuned PD (bootstrap p<0.01, monkeys a and b only).

Reference List

1. Scott,S.H. Apparatus for measuring and perturbing shoulder and elbow joint positions and torques during reaching. *J. Neurosci. Methods* **89**, 119-127 (1999).

2. Scott,S.H., Gribble,P.L., Graham,K.M. & Cabel,D.W. Dissociation between hand motion and population vectors from neural activity in motor cortex. *Nature* **413**, 161-165 (2001).

3. Sergio,L.E. & Scott,S.H. Hand and joint paths during reaching movements with and without vision. *Exp. Brain Res.* **122**, 157-164 (1998).

4. Loeb,G.E. & Gans,C. Electromyography for Experimentalists. The University of Chicago Press, Chicago (1986).

5. Scott,S.H. & Kalaska,J.F. Reaching movements with similar hand paths but different arm orientations. I. Activity of individual cells in motor cortex. *J. Neurophysiol.* **77**, 826-852 (1997).

6. Cabel, D.W., Cisek, P. & Scott, S.H. Neural activity in primary motor cortex related to mechanical loads applied to the shoulder and elbow during a postural task. *J. Neurophysiol.* **86**, 2102-2108 (2001).

7. Buchanan, T.S., Rovai, G.P. and Rymer, W.Z. Strategies for muscle activation during isometric torque generation at the human elbow. *J. Neurophysiol.* **62**, 1201-1212, (1989).

8. Hoffman, D.S. and Strick, P.L. Step-tracking movements of the wrist. IV. Muscle activity associated with movements in different directions. *J. Neurophysiol.* **81**, 319-333, (1999).
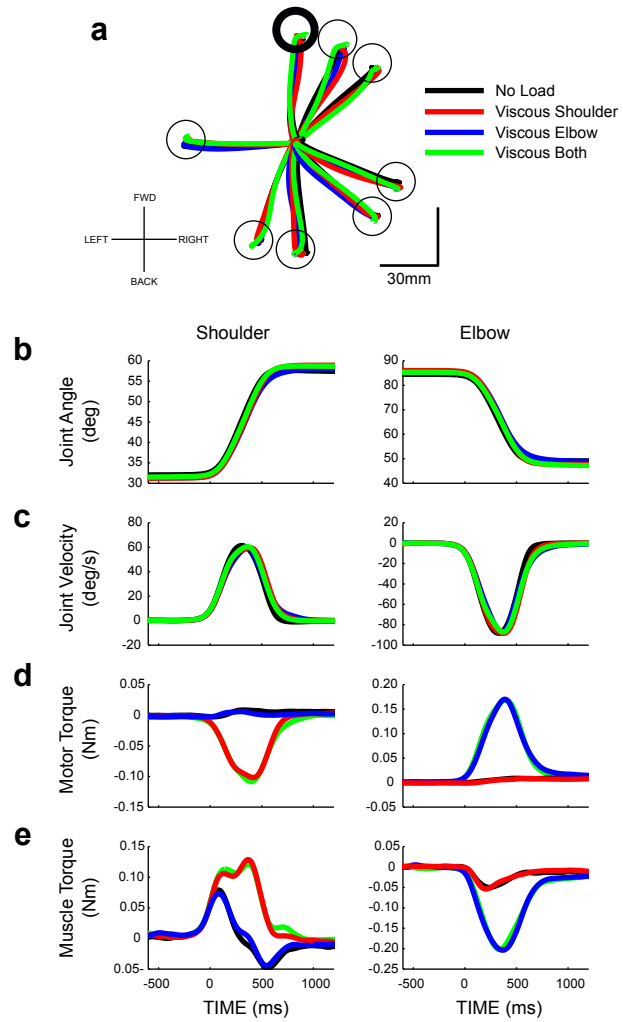
Table S1: Changes in shoulder and elbow muscle activity between unloaded reaching and reaching with loads applied to the shoulder (VS), elbow (VE) and both (VB) joints. Significant increases (+) and decreases (-) in activity are separated for each loading condition (ANOVA, $p < 0.05$ with Bonferroni corrections, see Methods).

	N	VB		VS		VE	
		(+)	(-)	(+)	(-)	(+)	(-)
mono	26	17	6	13	5	13	7
bi-art	14	8	1	7	4	8	2
mono	17	16	1	4	1	11	1

mono sho (PM,AD,MD,PD,Sp,Sb,TM,I,)
bi-art (SB,LB,LoT,De)
mono elb (B,Br,LaT,MT)

a

No Load
Viscous Shoulder
Viscous Elbow
Viscous Both

FWD
LEFT — RIGHT
BACK

30mm

Shoulder   Elbow

b Joint Angle (deg)

c Joint Velocity (deg/s)

d Motor Torque (Nm)

e Muscle Torque (Nm)

TIME (ms)   TIME (ms)

Gribble & Scott Fig. S1
Reference #S10669B HP/sbm

a

shoulder
elbow

0°

1 rad/sec

b

n=77

0°

c

n=46

0°

Gribble & Scott Fig.S2
Reference #S10669B HP/sbm